

Infrared features of the ghost propagators in quenched and unquenched lattice Landau gauge QCD

Hideo Nakajima, * Department of Information science,
Utsunomiya University

Sadataka Furui, † School of Science and Engineering,
Teikyo University

31 October 2006, JPS APS joint meeting

*e-mail nakajima@is.utsunomiya-u.ac.jp

†e-mail furui@umb.teikyo-u.ac.jp

Contents

- I. Introduction
- II. Color confinement
- III. The lattice Landau gauge
- IV. The Kugo-Ojima theory and the Zwanziger theory
- V. The ghost propagator
- VI. Summary and discussion

References: Phys. Rev. **D73**, 094506(2006), **D73**, 074503(2006),
D70, 094504(2004), **D69**, 074505(2004),
Few Body Systems**42**(2006): hep-lat/0503029
Brazilian Journal of Physics (IRQCD in Rio)(2006), hep-lat/0609024

I. Introduction

- Unquenched lattice Landau gauge simulation using MILC Asqtad Kogut-Susskind fermions.
- Color confinement
 - The Kugo-Ojima confinement parameter c .
 - A^2 condensate in running coupling, gluon propagator and quark propagator.
 - Ghost condensate parameter v and Binder cumulant of the color anti-symmetric ghost propagator.
- Dynamical chiral symmetry breaking

II. Color Confinement

- Kugo-Ojima theory based on the Lagrangian satisfying BRST symmetry yields a confinement criterion (A two-point function at $q = 0$). (Kugo-Ojima 1979)
- Gribov-Zwanziger theory gives a sufficient condition of the confinement for infrared exponents of gluon propagator and ghost propagator.(Gribov 1978, Zwanziger 1991)
- The lattice simulation of running coupling $\alpha_s(q)$ in \widetilde{MOM} scheme suggests presence of mass-dimension 2 (A^2) condensates.(Boucaud et al. 2000)

- The mass-dimension 2 condensates can be related to Zwanziger's horizon condition generated by restriction of the gauge field in fundamental modular region.(Dudal et al. 2005)
- The A^2 is not BRST invariant. A mixed condensate with $\bar{c}c$ becomes on-shell BRST invariant.(Kondo 2003)
- Local Composite Operator(LCO) approach suggests that $\bar{c}c$ condensate manifest itself in the color anti-symmetric ghost propagator. (Dudal et al. 2005)
- Investigation of the ghost condensate in SU(2) lattice Landau gauge was performed.(Cucchieri et al. 2005)

- The Kugo-Ojima confinement criterion:

$$\begin{aligned}
 & (\delta_{\mu\nu} - \frac{q_\mu q_\nu}{q^2}) u^{ab}(q^2) \\
 &= \frac{1}{V} \sum_{x,y} e^{-ip(x-y)} \langle \text{tr} \left(\Lambda^{a\dagger} D_\mu \frac{1}{-\partial D} [A_\nu, \Lambda^b] \right)_{xy} \rangle.
 \end{aligned}$$

The fact that the parameter c defined as $u^{ab}(0) = -\delta^{ab}c$ becomes 1 is the confinement criterion.

- The parameter c is related to the renormalization factor as

$$1 - c = \frac{Z_1}{Z_3} = \frac{\tilde{Z}_1}{\tilde{Z}_3} = \frac{Z_1^\psi}{Z_2}$$

- If the finiteness of \tilde{Z}_1 is proved, divergence of \tilde{Z}_3 is a sufficient condition. If Z_3 vanishes in the infrared, Z_1 should have higher order 0. If Z_2 is finite Z_1^ψ should vanish.

- Zwanziger's horizon condition

$$\sum_{x,y} e^{-ip(x-y)} \left\langle \text{tr} \left(\Lambda^{a\dagger} D_\mu \frac{1}{-\partial D} (-D_\nu) \Lambda^b \right)_{xy} \right\rangle \\ = G_{\mu\nu}(p) \delta^{ab} = \left(\frac{e}{d} \right) \frac{p_\mu p_\nu}{p^2} \delta^{ab} - \left(\delta_{\mu\nu} - \frac{p_\mu p_\nu}{p^2} \right) u^{ab},$$

where, with use of the covariant derivatitative $D_\mu(U)$

$$D_\mu(U_{x,\mu})\phi = S(U_{x,\mu})\partial_\mu\phi + [A_{x,\mu}, \bar{\phi}],$$

$$\partial_\mu\phi = \phi(x+\mu) - \phi(x), \text{ and } \bar{\phi} = \frac{\phi(x+\mu) + \phi(x)}{2}$$

$$e = \left\langle \sum_{x,\mu} \text{tr}(\Lambda^{a\dagger} S(U_{x,\mu}) \Lambda^a) \right\rangle / \{(N_c^2 - 1)V\}.$$

- The horizon condition reads $\lim_{p \rightarrow 0} G_{\mu\mu}(p) - e = 0$, and the l.h.s. of the condition is $\left(\frac{e}{d}\right) + (d-1)c - e = (d-1)h$ where $h = c - \frac{e}{d}$ and dimension $d = 4$, and it follows that $h = 0 \rightarrow$ horizon condition, and thus the horizon condition coincides with Kugo-Ojima criterion provided the covariant derivative approaches the naive continuum limit, i.e., $e/d = 1$.
- The renormalization group flow of the ghost propagator is assumed to follow perturbative renormalization-group flow equation.
- Suppression of the infrared modes of the gauge field corresponds to the vanishing of the gluon propagator.

III. The lattice Landau gauge

- Two types of the gauge field definitions:

1. log U type: $U_{x,\mu} = e^{A_{x,\mu}}$, $A_{x,\mu}^\dagger = -A_{x,\mu}$,

2. U linear type: $A_{x,\mu} = \frac{1}{2}(U_{x,\mu} - U_{x,\mu}^\dagger)|_{trlp.}$,

$$(A_\mu(x) = i \sum_a A_\mu^a(x) \frac{\Lambda^a}{\sqrt{2}}, \quad \text{tr} \Lambda^a \Lambda^b = \delta^{ab})$$

- The optimizing function

1. $F_U(g) = \|A^g\|^2 = \sum_{x,\mu} \text{tr} (A^g_{x,\mu}^\dagger A^g_{x,\mu})$,

2. $F_U(g) = \sum_{x,\mu} \text{tr} (2 - (U^g_{x,\mu} + U^g_{x,\mu}^\dagger))$,

- Under infinitesimal gauge transformation $g^{-1}\delta g = \epsilon$, its variation reads for either definition as

$$\Delta F_U(g) = -2\langle \partial A^g | \epsilon \rangle + \langle \epsilon | -\partial D(U^g) | \epsilon \rangle + \dots,$$

- Stationarity(Landau gauge), Local minimum(Gribov Region), Global minimum(Fundamental modular(FM) region)

Kugo-Ojima parameter c of quenched SU(3)

U -linear(left) and $\log U$ (right). $\beta = 6.0$ and 6.4 .

β	L	c_1	e_1/d	h_1	c_2	e_2/d	h_2
6.0	16	0.576(79)	0.860(1)	-0.28	0.628(94)	0.943(1)	-0.32
6.0	24	0.695(63)	0.861(1)	-0.17	0.774(76)	0.944(1)	-0.17
6.0	32	0.706(39)	0.862(1)	-0.15	0.777(46)	0.944(1)	-0.16
6.4	32	0.650(39)	0.883(1)	-0.23	0.700(42)	0.953(1)	-0.25
6.4	48	0.739(65)	0.884(1)	-0.15(7)	0.793(61)	0.954(1)	-0.16
6.4	56	0.758(52)	0.884(1)	-0.13(5)	0.827(27)	0.954(1)	-0.12
6.45	56				0.814(89)	0.954(1)	-0.14

MILC configurations used in our simulation

	β_{imp}	am_{ud}^{VWI}/am_s^{VWI}	N_f	$1/a(\text{GeV})$	L_s	L_t	$aL_s(\text{fm})$
MILC_c	6.83	0.040/0.050	2+1	1.64	20	64	2.41
	6.76	0.007/0.050	2+1	1.64	20	64	2.41
MILC_f	7.11	0.0124/0.031	2+1	2.19	28	96	2.52
	7.09	0.0062/0.031	2+1	2.19	28	96	2.52
MILC_{ft}	5.65	0.008	2	1.716	24	12	2.76
	5.725	0.008	2	1.914	24	12	2.47
	5.85	0.008	2	2.244	24	12	2.11

The Kugo-Ojima parameter of unquenched SU(3)

Table 1: The Kugo-Ojima parameter for the polarization along the spacial directions c_x and that along the time direction c_t and the average c , trace divided by the dimension e/d , horizon function deviation h of the unquenched KS fermion ($\text{MILC}_c, \text{MILC}_f, \text{MILC}_{ft}$) with use of $\log U$ definition.

	β_{imp}	c_x	c_t	c	e/d	h
MILC_c	6.76	1.04(11)	0.74(3)	0.97(16)	0.9325(1)	0.03(16)
	6.83	0.99(14)	0.75(3)	0.93(16)	0.9339(1)	-0.00(16)
MILC_f	7.09	1.06(13)	0.76(3)	0.99(17)	0.9409(1)	0.04(17)
	7.11	1.05(13)	0.76(3)	0.98(17)	0.9412(1)	0.04(17)
MILC_{ft}	5.65	0.72(13)	1.04(23)	0.80(21)	0.9400(7)	-0.14
	5.725	0.68(15)	0.77(16)	0.70(15)	0.9430(2)	-0.24
	5.85	0.63(19)	0.60(12)	0.62(17)	0.9465(2)	-0.33

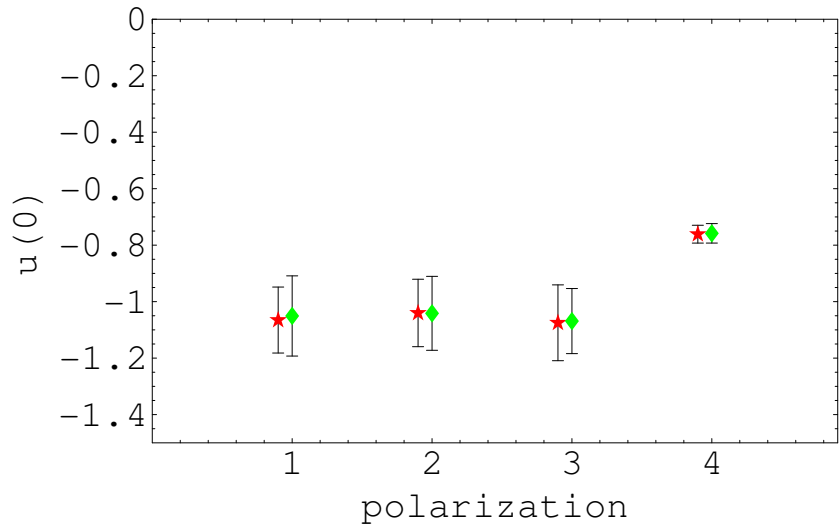


Fig. 1: Kugo-Ojima parameter $u(0)$ of MILC_f $N_f = 2 + 1$ KS fermion unquenched configurations of $\beta_{imp} = 7.11$ (green diamonds), $\beta_{imp} = 7.09$ (red stars) .

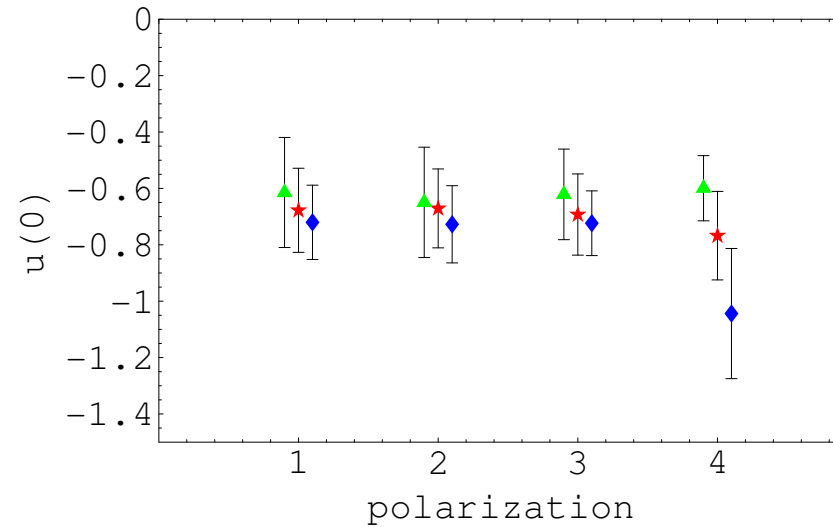


Fig. 2: Kugo-Ojima parameter $u(0)$ of MILC finite temperature configurations of $\beta = 5.65$ (blue diamonds), $\beta = 5.725$ (red stars) and $\beta = 5.85$ (green triangles).

IV. The Ghost propagator

$$\begin{aligned} FT[D_G^{ab}(x, y)] &= FT\langle \text{tr}(\Lambda^a \{(\mathcal{M}[U])^{-1}\}_{xy} \Lambda^b) \rangle, \\ &= \delta^{ab} D_G(q^2), \end{aligned}$$

$$\mathcal{M} = -\partial_\mu D_\mu.$$

- Ghost dressing function $G(q^2) = q^2 D_G(q^2)$.
- Solve the equation with plane wave sources.

$$-\partial_\mu D_\mu f_s^b(\mathbf{x}) = \frac{1}{\sqrt{V}} \Lambda^b \sin \mathbf{q} \cdot \mathbf{x} \quad (1)$$

$$-\partial_\mu D_\mu f_c^b(\mathbf{x}) = \frac{1}{\sqrt{V}} \Lambda^b \cos \mathbf{q} \cdot \mathbf{x}. \quad (2)$$

- Color diagonal ghost propagator

$$D_G(q) = \frac{1}{N_c^2 - 1} \frac{1}{V} \times \delta^{ab} (\langle \Lambda^a \cos \mathbf{q} \cdot \mathbf{x} | f_c^b(\mathbf{x}) \rangle + \langle \Lambda^a \sin \mathbf{q} \cdot \mathbf{x} | f_s^b(\mathbf{x}) \rangle) \quad (3)$$

- Color anti-symmetric ghost propagator

$$\phi^c(q) = \frac{1}{\mathcal{N}} \frac{1}{V} \times f^{abc} (\langle \Lambda^a \cos \mathbf{q} \cdot \mathbf{x} | f_s^b(\mathbf{x}) \rangle - \langle \Lambda^a \sin \mathbf{q} \cdot \mathbf{x} | f_c^b(\mathbf{x}) \rangle) \quad (4)$$

where $\mathcal{N} = 2$ for $SU(2)$ and 6 for $SU(3)$.

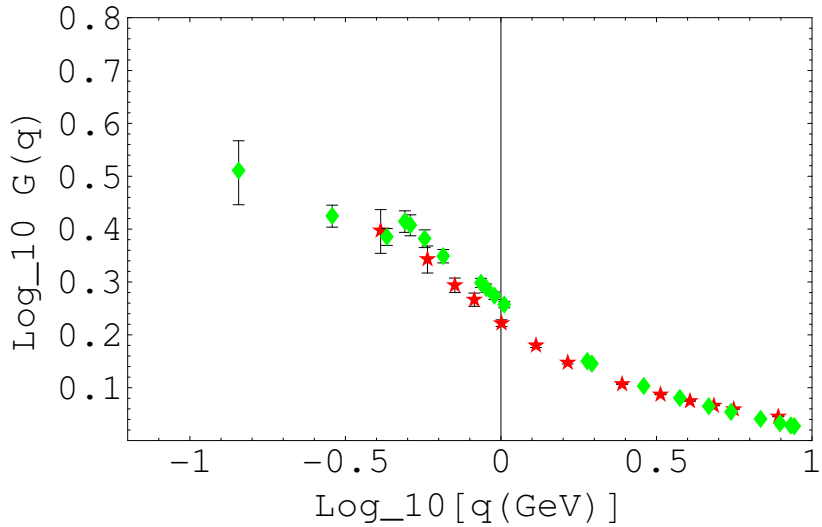


Fig. 3: Log of the ghost dressing function $\log_{10} G(q)$ as a function of $\log_{10} q(\text{GeV})$ of $\text{MILC}_f \beta_{imp} = 7.09$ (diamonds) and that of quenched $\beta = 6.45\ 56^4$ (stars).

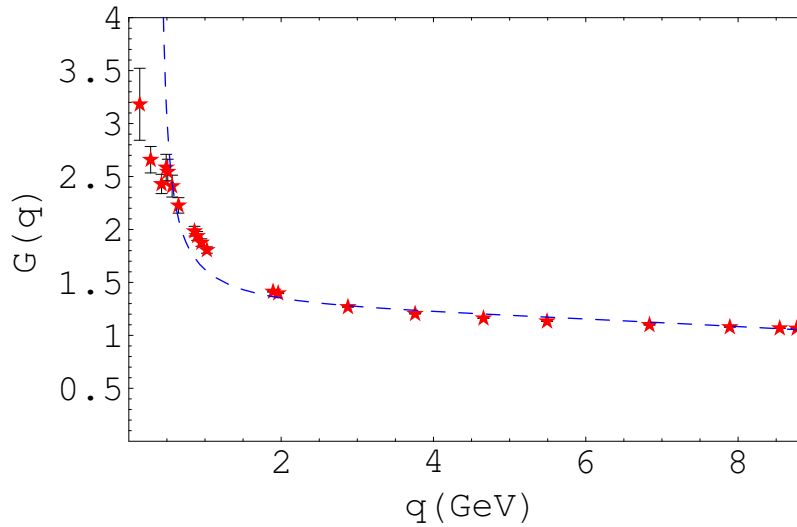


Fig. 4: The ghost dressing function of $\text{MILC}_f \beta_{imp} = 7.09$ (stars) Dashed line is the 4-loop $N_f = 2$ pQCD result ($\lambda_G = 3.01, y = 0.0246100$)

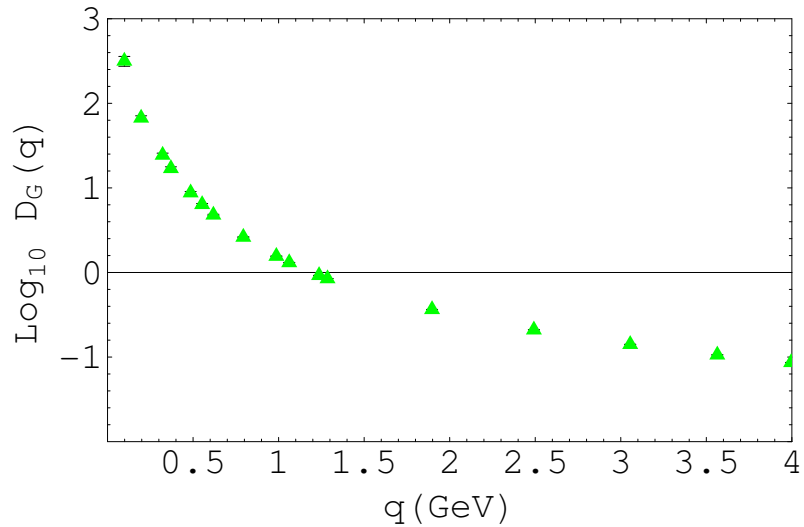


Fig. 5: Log of the color diagonal ghost propagator of $\log_{10}[D_G(q)]$ as a function of $q(\text{GeV})$ MILC_c.

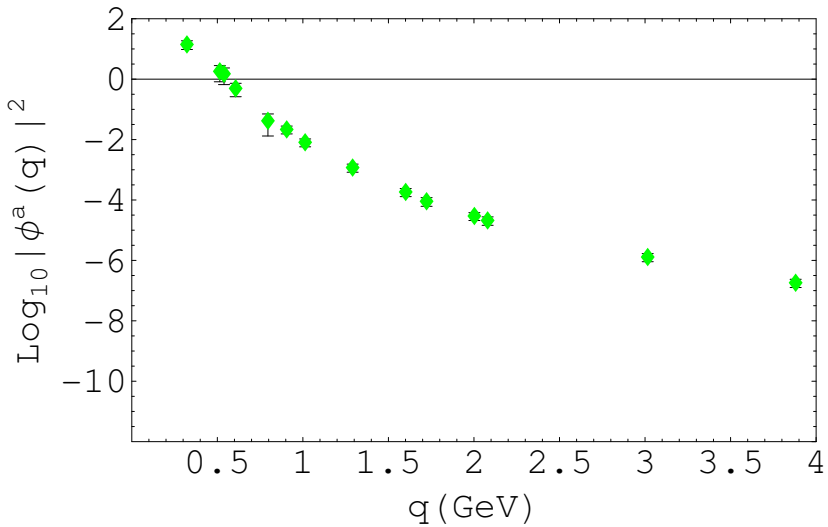


Fig. 6: Log of the color anti-symmetric ghost propagator squared $\log_{10}[\phi(q)^2]$ as a function of $q(\text{GeV})$. $20^3 \times 64$ MILC_c.

The ghost condensate

- The ghost condensate $\langle f^{abc} \bar{c}^b c^c \rangle$ in the color anti-symmetric ghost propagator is parametrized by v , r and z .
- Expression of the finite size effect in the $L_x^3 L_t$ lattice for q_μ under cylinder cut is difficult. Our choice is,

$$\frac{1}{N_c^2 - 1} \sum_a \frac{\sqrt{L_x^3 L_t}}{\cos(\pi \tilde{q}/8\sqrt{L_x L_t})} \langle |\phi^a(q)| \rangle = \frac{r}{q^z}, \quad (5)$$

$$\tilde{q}^2 = \sum_{i=1}^3 (2 \sin \frac{\pi \bar{q}_i}{L_x})^2 + (2 \sin \frac{\pi \bar{q}_4}{L_t})^2 \quad (6)$$

$$\frac{1}{N_c^2 - 1} \sum_a \langle |\phi^a(q)| \rangle = \frac{r/\sqrt{L_x^3 L_t} + v}{q^4 + v^2} \quad (7)$$

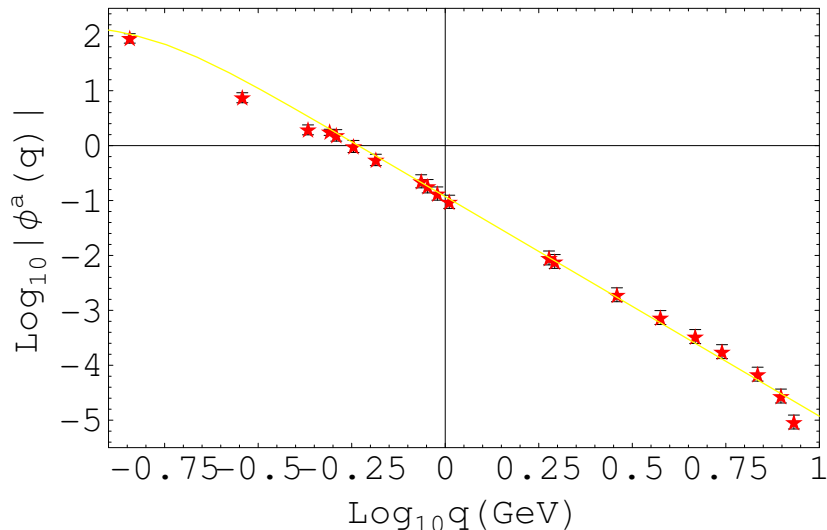


Fig. 7: The logarithm of the color antisymmetric ghost propagator of MILC_f as the function of $\log_{10}(q(\text{GeV}))$ and the fit using $r = 134$ and $v = 0.026\text{GeV}^2$.

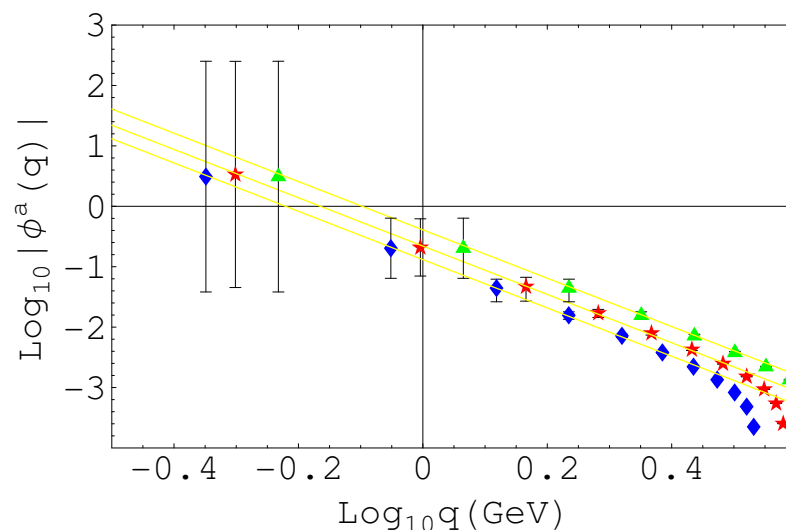


Fig. 8: The logarithm of the color antisymmetric ghost propagator of MILC_{ft} of $T = 143\text{MeV}$ (blue diamonds), $T = 159.5\text{MeV}$ (red stars) and $T = 187\text{MeV}$ (green triangles) and their fits.

The Binder cumulant

- Binder cumulant of the color antisymmetric ghost propagator

$$U(q) = 1 - \frac{\langle \vec{\phi}(q)^4 \rangle}{3\langle \vec{\phi}(q)^2 \rangle^2}.$$

- Suppression away from the d-dimensional gaussian distribution $\frac{\langle \vec{\phi}^4 \rangle}{(\langle \vec{\phi}^2 \rangle)^2} = \frac{d+2}{d}$ may imply presence of ghost condensate.

- Quenched SU(2) is compatible with gaussian. MILC_c shows a larger randomness than the Gaussian.

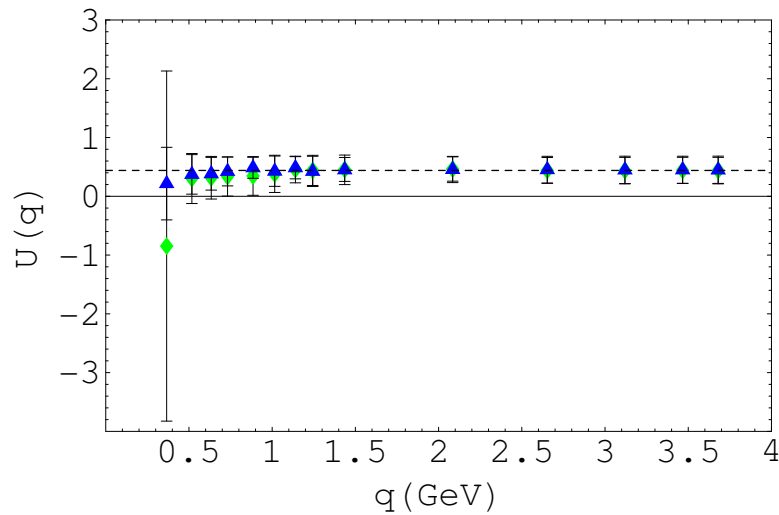


Fig. 9: The momentum dependence of Binder cumulant $U(q)$ of $SU(2)$, $\beta = 2.2$, $a = 1.07\text{GeV}^{-1}$ of PT samples(blue triangles) and first copy samples(green diamonds).

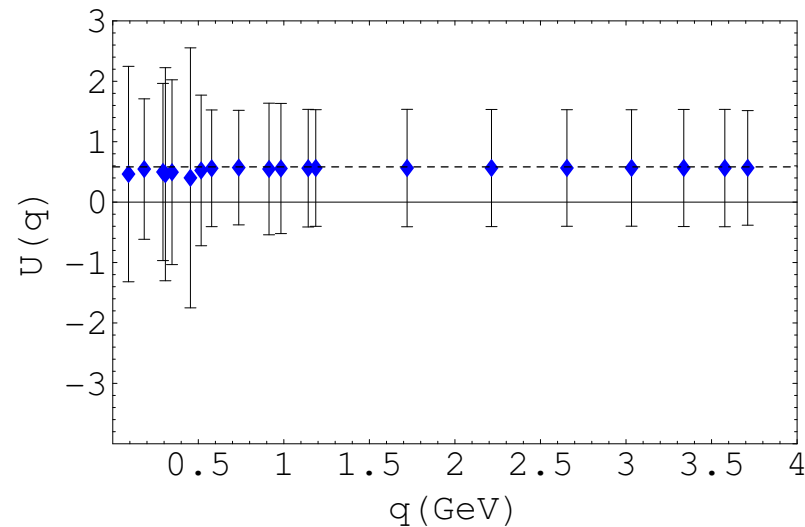


Fig.10: The momentum dependence of Binder cumulant $U(q)$ of unquenched $SU(3)$, $a = 1.64\text{GeV}^{-1}$ MILC_c.

Exceptional samples

- In $\beta = 6.4, 56^4$ quenched SU(3) configurations, we found a copy whose $\alpha_G = 0.272$ v.s. $\alpha_G(\text{average})=0.223$, and whose gluon propagator has an axis along which the reflection positivity is manifestly violated.
- In the $\beta_{imp} = 6.76, 20^3 \times 64$ MILC_c configurations (21 samples), we find a similar exceptional sample.
- The exceptional sample makes the sample average of the Binder cumulant of color anti-symmetric ghost propagator in the infrared small, and the standard deviation large.

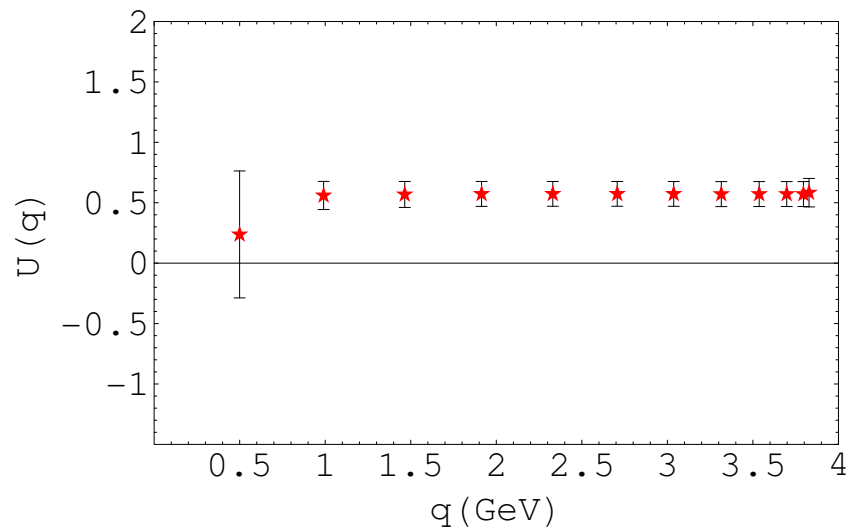


Fig.11: The Binder cumulant of the color antisymmetric ghost propagator of MILC_{ft} $N_f = 2$ configurations of $\beta = 5.725$ (red stars)

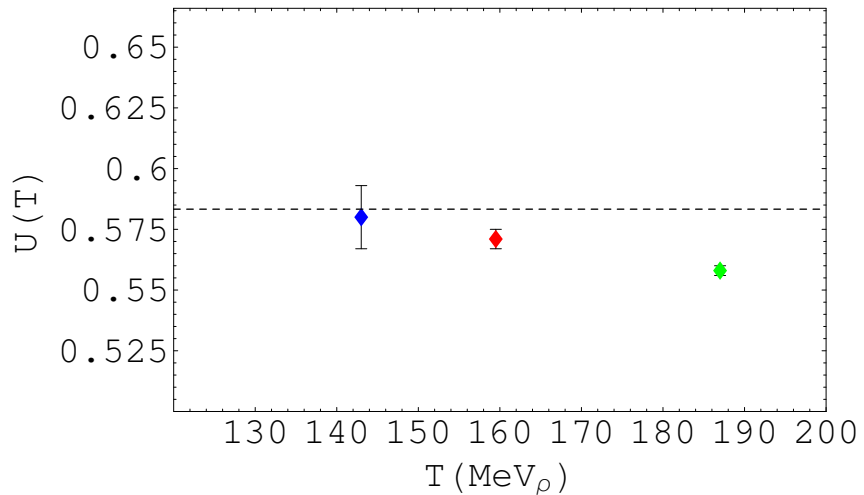


Fig.12: Averages over momenta excluding the lowest momentum point of the Binder cumulants of MILC finite temperature configurations. $\beta = 5.65$ (blue diamonds), $\beta = 5.725$ (red stars) and $\beta = 5.85$ (green triangles).

- The fitted parameters r, z, v of $|\phi(q)|$, $\bar{r}, \bar{z}, \bar{v}$ of $\phi(q)^2$ and U of MILC_c and MILC_f samples. (U of MILC_f corresponds to the average below $q = 1\text{GeV}$ and the average above 1GeV , respectively)

β_{imp}	$m_0(\text{MeV})$	r	z	v	\bar{r}	\bar{z}	\bar{v}	U
6.76	11.5/82.2	37.5	3.90	0.012	33.5	7.6	0.045	0.53(5)
6.83	65.7/82.2	38.7	3.85	0.007	33.5	7.6	0.048	0.57(4)
7.09	13.6/68.0	134	3.83	0.026	251	7.35	0.044	0.57(4)/0.56(1)
7.11	27.2/68.0	112	3.81	0.028	164	7.34	0.002	0.58(2)/0.52(1)

- The data of MILC_f $\beta_{imp} = 7.11$ are rather noisy. $U(q)$ below 1GeV and above 1GeV are different. The anomaly is correlated with that of the dynamical quark mass function.

The infrared exponents of ghost and gluon

	β/β_{imp}	α_G	α_D	$\alpha_D + 2\alpha_G$
quench	6.40	0.22	-0.32	0.12
MILC _c	6.76	0.25	-0.60	-0.10
	6.83	0.23	-0.57	-0.11
MILC _f	7.09	0.24	-0.67	-0.19
	7.11	0.23	-0.65	-0.19

VII. The quark propagator

- The statistical average over Landau-gauge-fixed samples

$$S_{\alpha\beta}(p) = \left\langle \langle \chi_{p,\alpha} | \frac{1}{i\cancel{D}(U) + m} | \chi_{p,\beta} \rangle \right\rangle$$

The inversion, $\frac{1}{i\cancel{D}(U) + m}$, is performed via conjugate gradient method after preconditioning.

$$S_{\alpha\beta}(q) = Z_2(q) \frac{-i\gamma q + M(q)}{q^2 + M(q)^2}$$

- The mass function in large q .

$$M(q) = -\frac{4\pi^2 d_M \langle \bar{\psi} \psi \rangle_\mu [\log(q^2/\Lambda_{QCD}^2)]^{d_M-1}}{3q^2 [\log(\mu^2/\Lambda_{QCD}^2)]^{d_M}} + \frac{m(\mu^2) [\log(\mu^2/\Lambda_{QCD}^2)]^{d_M}}{[\log(q^2/\Lambda_{QCD}^2)]^{d_M}},$$

$$d_M = 12/(33 - 2N_f)$$

- The mass function in the infrared region.

$$M(q) = \frac{\tilde{c}\Lambda^3}{q^2 + \Lambda^2} + m_0$$

The mass function

The parameters \tilde{c} and Λ of the Staple+Naik action(left) and the Asqtad action.

β_{imp}	$m_0(\text{MeV})$	\tilde{c}	$\Lambda(\text{GeV})$	$\tilde{c}\Lambda(\text{GeV})$	\tilde{c}	$\Lambda(\text{GeV})$	$\tilde{c}\Lambda(\text{GeV})$
6.76	11.5	0.44(1)	0.87(2)	0.38	0.45(1)	0.91(2)	0.41
	82.2	0.30(1)	1.45(2)	0.43	0.33(1)	1.36(1)	0.46
6.83	65.7	0.33(1)	1.28(2)	0.42	0.35(1)	1.25(1)	0.44
	82.2	0.30(1)	1.45(2)	0.43	0.33(1)	1.34(1)	0.45
7.09	13.6	0.45(1)	0.82(2)	0.37	0.50(2)	0.79(2)	0.39
	68.0	0.30(1)	1.27(4)	0.38	0.35(1)	1.19(1)	0.41
7.11	27.2	0.43(1)	0.89(2)	0.38	0.20(2)	1.04(3)	0.21
	68.0	0.32(1)	1.23(2)	0.40	0.36(1)	1.15(1)	0.42

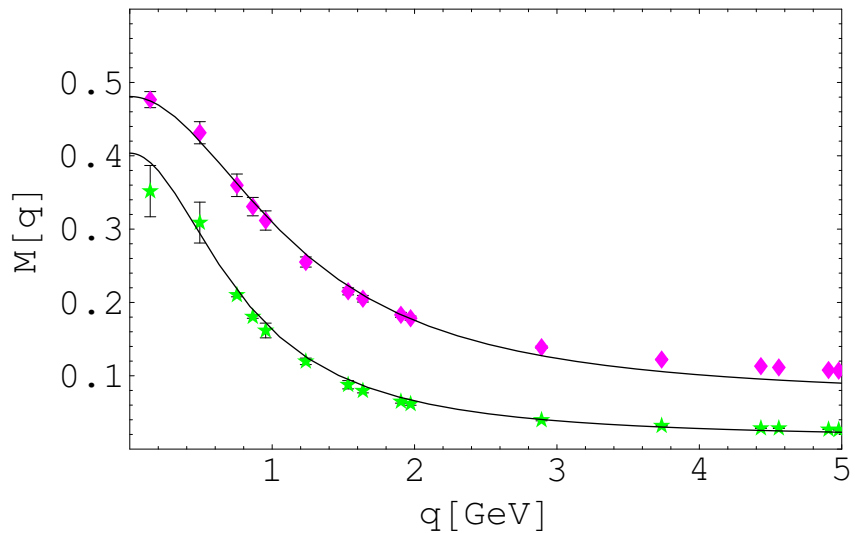


Fig.13: The mass function $M(q)$ of the Asqtad action of MILC_f with the bare quark mass $m_0 = 13.6\text{MeV}$ (green stars) and with the bare quark mass $m_0 = 68\text{MeV}$ (red diamonds).

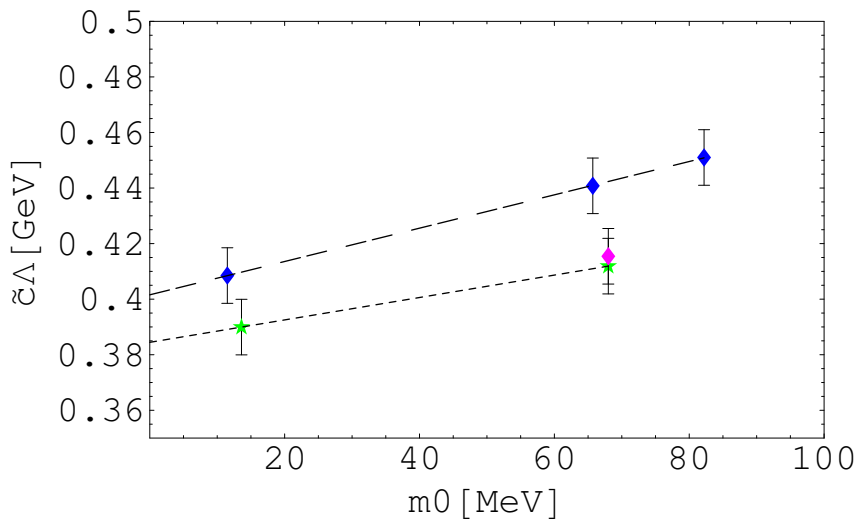


Fig.14: The chiral symmetry breaking mass $\tilde{\Lambda}$ as a function of bare mass and its chiral limit. Dotted line is an extrapolation of MILC_f and the dash-dotted line is that of MILC_c , Asqtad action.

VIII. Summary and Discussion

- The Kugo-Ojima parameter c saturated at about 0.8 in the quenched 56^4 lattice, but it is consistent with 1 in the zero temperature MILC configurations.
- The quark has the effect of quenching randomness.
- The condensate parameter v in the color anti-symmetric ghost propagator in quenched SU(2) is consistent with 0 and also small in MILC_c and MILC_f .
- The Binder cumulants of zero temperature MILC are close to those of Gaussian distributions except the lowest momentum point.
- The Binder cumulants of MILC finite temperature($T > T_c$) show larger randomness than those of Gaussian distributions.

- The gluon propagator is infrared finite?
- Kugo-Ojima confinement criterion
 - * $\frac{Z_1}{Z_3} = \frac{o((q^2)^{-\alpha_D+s})}{O((q^2)^{-\alpha_D})}$ [$s > 0$]?
 - * $\frac{\tilde{Z}_1}{\tilde{Z}_3} = \frac{1}{\infty}$
 - * $\frac{Z_1^\psi}{Z_2} = \frac{o((q^2)^s)}{O(1)}$ [$s > 0$]?
- How does the true vacuum manifest itself in the $V \rightarrow \infty$ limit of the simulation?

References

- [1] T. Kugo and I. Ojima, Prog. Theor. Phys. Suppl. **66**, 1 (1979).
- [2] V.N. Gribov, Nucl. Phys. **B 139** 1(1978).
- [3] D. Zwanziger, Nucl. Phys. **B 364** ,127 (1991), idem **B 412**, 657 (1994).
- [4] P.O. Bowman et al., Phys. Rev. **D71**,054507(2005).
- [5] A. Cucchieri, Nucl. Phys. **B521**,365(1998).
- [6] A. Cucchieri, T. Mendes and A. Mihara, Phys. Rev. **D72**,094505(2004).
- [7] Ph. Boucaud et al., hep-lat/0504017.

- [8] S. Furui and H.Nakajima, Phys. Rev. D**69**,074505(2004), hep-lat/0305010.
- [9] S. Furui and H.Nakajima, Phys. Rev. D**70**,094504(2004), hep-lat/0403021.
- [10] S. Furui and H. Nakajima, Few Body Systems**42**(2006), hep-lat/0503029.
- [11] H. Nakajima and S. Furui, PoS **LAT2005** 302 (2005),hep-lat/0509033.
- [12] S. Furui and H. Nakajima, PoS **LAT2005** 291 (2005),hep-lat/0509035.
- [13] S. Furui and H. Nakajima, Phys. Rev. D**73**,074503(2006),hep-lat/0511045.
- [14] S. Furui and H. Nakajima, Phys. Rev. D**73**,094506(2006),hep-lat/0602027.